

Josephson diode effect in a ballistic single-channel nanowire

Julia S. Meyer¹ and Manuel Houzet¹

Univ. Grenoble Alpes, CEA, Grenoble INP, IRIG, PHELIQS, 38000 Grenoble, France

(*Electronic mail: julia.meyer@univ-grenoble-alpes.fr.)

(Dated: 22 July 2024)

When time-reversal and inversion symmetry are broken, superconducting circuits may exhibit a so-called diode effect, where the critical currents for opposite directions of the current flow differ. In recent years, this effect has been observed in a multitude of systems and the different physical ingredients that may yield such an effect are well understood. On a microscopic level, the interplay between spin-orbit coupling and a Zeeman field may give rise to a diode effect in a single Josephson junction. However, so far there is no analytical description of the effect within a simple model. Here we study a single channel nanowire with Rashba spin-orbit coupling and in the presence of a Zeeman field. We show that the different Fermi velocities and spin projections of the two pseudo-spin bands lead to a diode effect. Simple analytical expressions for the diode efficiency can be obtained in limiting cases.

The so-called superconducting diode effect has attracted a lot of attention recently^{1,2}. In systems breaking inversion and time-reversal symmetry, the critical currents in opposite directions may be different. Experimentally this has been observed in a variety of bulk superconductors³⁻⁷, as well as in circuits containing Josephson junctions⁸⁻¹⁵. One of the possible origins of the diode effect in Josephson junctions is the interplay between Rashba spin-orbit coupling and an external magnetic field¹⁶⁻¹⁸. The diode effect is then linked to the so-called ϕ_0 -junction behavior^{16,17,19-21}, where the current phase-relation acquires a field-tunable phase shift and an anomalous supercurrent flows in the absence of a phase bias. The simplest current-phase relation yielding these effects is $I = I_{c1} \sin(\phi - \phi_0)$. By contrast, the diode effect requires a current-phase relation with more than one harmonic. The simplest case is provided by the presence of a second harmonic, $I_{c2} \sin(2\phi - \phi_0)$, with a phase shift $\phi_0 \neq 2\phi_0$. While such a phenomenological current-phase relation has been used in the literature^{9,22,23}, a microscopic derivation has been missing. Here we show that, in ballistic single-channel Josephson junctions, such a current-phase relation can indeed be realized, both in short and long junctions at finite temperature, thus allowing one to characterize their diode efficiency. In this paper, we will concentrate on the cases where analytical results are available.

We consider a simple 2D model of a nanowire with Rashba spin-orbit coupling^{24,25} in the presence of an external magnetic field. Due to the Rashba spin-orbit coupling, an electric field perpendicular to the plane generates an effective spin-orbit magnetic field in the plane and perpendicular to the nanowire. A diode effect may arise if the external magnetic

field is aligned with the spin-orbit field.

A single channel with different Fermi velocities, $v_j = \bar{v} + j\delta v/2$, and Zeeman energies, $h_j = \bar{h} + j\delta h/2$, resulting from different spin projections, for the two pseudo-spin bands $j = \pm$, see Fig. 1, requires at least one of two ingredients (see Supplementary Material): a finite transverse width such that the spin-orbit coupling associated with the transverse motion comes into play or a magnetic field \vec{h}_\perp transverse to the spin-orbit field. In the former case, $\delta v/\bar{v} \sim E_{so}^{5/2} \sqrt{\bar{\mu}}/\omega_0^3$, whereas $\delta h/\bar{h} \sim E_{so}^{3/2} \sqrt{\bar{\mu}}/\omega_0^2$ is typically larger. Here $E_{so} = m\alpha^2/2$ is the spin-orbit energy associated with the Rashba coupling α and m is the effective electron mass, while $\bar{\mu}$ is an effective chemical potential and ω_0 is the energy scale associated with the transverse confining potential. In the latter case, the difference in Fermi velocities and effective fields is determined by $\delta v/\bar{v}, \delta h/\bar{h} \sim h_\perp^2/(\sqrt{E_{so}}\bar{\mu}^{3/2})$. The field \vec{h}_\perp may be chosen along the nanowire, which is the direction considered in order to realize topological superconductivity with Majorana end modes in proximitized nanowires^{26,27}. When superconductivity is induced, h_\perp also modifies the induced gaps $\Delta_j = \bar{\Delta} + j\delta\Delta/2$ in such a way that $\Delta_-/\Delta_+ = h_-/h_+$ ²⁸.

We neglect the orbital effect, which is expected to be small as long as $h \ll g\mu_B\Phi_0/(ad)$, where g is the g -factor, μ_B the Bohr magneton, Φ_0 the flux quantum, and a is the extension of the wavefunction in the direction perpendicular to the plane. Furthermore, the relevant length d is set by the smaller of the coherence length $\xi = \bar{v}/\bar{\Delta}$ or the length of the junction L . As the enhancement of the g -factor induced by spin-orbit coupling compensates an associated reduction of the effective mass, the above condition at the field that optimizes the diode effect $h \sim \Delta$ for the effect due to the reservoirs and $h \sim \bar{v}/L$ for the effect due to the normal part of the junction, see below) reduces to $a \ll \lambda_F$, where $\lambda_F = 2\pi/(m\bar{v})$ is the Fermi wavelength; it is fulfilled in a semiconducting nanowire at low density²⁹. (We use units where $\hbar = k_B = 1$.)

Linearizing the spectrum close to the Fermi level, one thus obtains an effective Hamiltonian

$$H_{\text{eff}}^N = \sum_{j=\pm} (jv_j p_x - h_j) \sigma_z - \bar{\mu}, \quad (1)$$

where p_x is the longitudinal momentum and σ_z is a Pauli matrix in pseudo-spin space. Adding superconductivity to de-

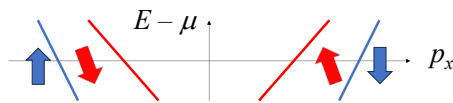


FIG. 1. Linearized band structure in the vicinity of the Fermi level. The $j = +$ band shown in blue and the $j = -$ band shown in red have different Fermi velocities as well as different spin projections.

scribe a Josephson junction, such that the normal part of the junction extends from $-L/2$ to $L/2$, one finds

$$H_{\text{eff}} = \sum_j [(jv_j p_x \sigma_z - \mu) \tau_z - h_j \sigma_z + \Delta_j \tau_+ + \Delta_j^* \tau_-], \quad (2)$$

where τ_i ($i = x, y, z$) are Pauli matrices in particle-hole space and $\tau_{\pm} = \tau_x \pm i\tau_y$. The spatial dependence of the Zeeman field and order parameter are given as $h_j(x) = h_j^N \theta(L/2 - |x|) + h_j^S \theta(|x| - L/2)$ and $\Delta_j(x) = \Delta_j \exp[i \text{sign}(x) \phi/2] \theta(|x| - L/2)$, where Δ_j and ϕ are the superconducting gaps of the two pseudo-spin bands and phase difference, respectively.³⁰ Here the magnetic field h_j^N in the junction and the magnetic field h_j^S in the superconducting leads may be different due to magnetic screening. Note that an homogeneous version of Eq. (2) may be used to analyze the ‘‘bulk’’ diode efficiency associated with the asymmetry of depairing currents in a 1D model of bulk superconductor^{31,32}.

Both fields h_j^N and h_j^S contribute to the Josephson diode effect^{28,33,34}. We obtain the supercurrent using Eq. (3) in Ref. 34 for a ballistic Josephson junction and summing over both pseudo-spin bands:

$$I_J = -4eT \frac{d}{d\phi} \Re \sum_{j=\pm; v \geq 0} \ln \left[1 + a_j^2(\omega_v) e^{-2\omega_v/E_{Lj}} e^{i(\phi + j\phi_j)} \right] / \quad (3)$$

Furthermore, $E_{Lj} = v_j/L$ and $\phi_j = 2h_j^N/E_{Lj}$ are Thouless energies and phase shifts associated with electron propagation in the normal region. $a_{\pm}(\omega_v) = (\omega_v \mp ih_{\pm}^S)/\Delta_{\pm} - [(\omega_v \mp ih_{\pm}^S)^2/\Delta_{\pm}^2 + 1]^{1/2}$ with the fermionic Matsubara frequencies $\omega_v = 2\pi T(v + 1/2)$ at temperature T accounts for scattering at the normal/superconductor interfaces. (Restituting k_B and \hbar , the prefactor yielding the current scale is given as $eT \rightarrow ek_B T/\hbar$.)

The critical currents for opposite current directions are defined as $I_c^> = \max_{\phi} I_J(\phi)$ and $I_c^< = -\min_{\phi} I_J(\phi)$. Then Eq. (3) allows one to obtain the diode efficiency $\eta = (I_c^> - I_c^<)/(I_c^> + I_c^<)$ for arbitrary fields, length of the junction, and temperature.

It turns out the diode effect due to the field in the junction behaves quite differently than the one due to the field in the leads. We will start by discussing the effect of the field in the junction only. To do so, we will assume that the magnetic field is confined to the junction. Then Eq. (3) simplifies to

$$I_J = \sum_{j=\pm; k>0} I_{kj} \sin(k(\phi + j\phi_j)) \quad (4)$$

with

$$I_{kj} = -4eT \sum_{v \geq 0} (-1)^k k a^{2k}(\omega_v) e^{-2k\omega_v/E_{Lj}}, \quad (5)$$

Here $a(\omega_v) = \omega_v/\Delta - [\omega_v^2/\Delta^2 + 1]^{1/2}$, where Δ is the common gap for both pseudo-spin bands.

In general, all harmonics contribute to the current-phase relation of a ballistic Josephson junction. Typically, the higher the harmonics, the stronger their suppression with temperature. When the two first harmonics dominate over the other

ones, the current-phase relation (4) can be rewritten in the form³⁵

$$I_J = I_{c1} \sin(\phi - \phi_0) + I_{c2} \sin(2(\phi - \phi_0) + \delta_{12}) \quad (6)$$

with

$$I_{ck} = \sqrt{I_{k+}^2 + I_{k-}^2 + 2I_{k+}I_{k-} \cos(k(\phi_+ + \phi_-))}, \quad (7)$$

$$\phi_{0k} = -\arctan \frac{I_{k+} \sin(k\phi_+) - I_{k-} \sin(k\phi_-)}{I_{k+} \cos(k\phi_+) + I_{k-} \cos(k\phi_-)}, \quad (8)$$

such that $\phi_0 = \phi_{01}$ and $\delta_{12} = 2\phi_{01} - \phi_{02}$. The diode efficiency is non-vanishing unless $I_{c1} = 0$ or $I_{c2} = 0$ or $\delta_{12} = 0 \text{ mod } \pi$. The maximal diode efficiency²³ $\eta_{\text{max}} = 1/3$ is achieved at $I_{c2} = I_{c1}/2$ and $\delta_{12} = \pi/2 \text{ mod } \pi$.

Typically $I_{c2} \ll I_{c1}$. Then the diode efficiency takes the simple form

$$\eta \approx -\frac{I_{c2}}{I_{c1}} \sin \delta_{12}. \quad (9)$$

The result can be further simplified introducing $I_{kj} = \bar{I}_k + j\delta I_k/2$ and $\phi_j = \bar{\phi} + j\delta\phi/2$. At weak spin-orbit coupling, $\delta v/\bar{v}, \delta h/\bar{h} \ll 1$ yields $\delta I_k \ll \bar{I}_k$ and $\delta\phi \ll \bar{\phi}$, such that $I_{ck} \approx 2\bar{I}_k |\cos(k\bar{\phi})|$ and

$$\phi_{0k} \approx -\left(\frac{k\delta\phi}{2} + \frac{\delta I_k}{2\bar{I}_k} \tan(k\bar{\phi}) \right). \quad (10)$$

Note that $\bar{\phi} = 2\bar{h}/\bar{E}_L$ with $\bar{E}_L = \bar{v}/L$ and $\delta\phi = (\delta h/\bar{h} - \delta v/\bar{v})\bar{\phi}/2$. If $\bar{\phi} \ll 1$, the diode efficiency is linear in the magnetic field and given as

$$\eta \approx \frac{\bar{I}_2}{\bar{I}_1} \left(\frac{\delta I_1}{\bar{I}_1} - \frac{\delta I_2}{\bar{I}_2} \right) \bar{\phi}. \quad (11)$$

If $\delta I_2/\bar{I}_2 = \delta I_1/\bar{I}_1$, a residual effect $\propto \bar{h}^3$ remains, namely $\eta \approx (\delta I_1/\bar{I}_1)\bar{\phi}^3$. As δ_{12} increases with \bar{h} , the diode efficiency changes sign at larger fields, when δ_{12} exceeds π , according to Eq. (9).

As we discuss below, a current-phase relation with essentially two harmonics may be realized in a junction with arbitrary length at $T_c - T \ll T_c$, where T_c is the critical temperature of the leads. In a long junction, lower temperatures $E_{Lj} \ll T \ll T_c$ are sufficient.

Near T_c , the gap Δ vanishes. Thus $\Delta \ll \omega_v$, such that $a(\omega_v) \approx -\Delta/(2\omega_v)$. As a consequence, $I_{kj} \propto \Delta^{2k}$ and we may keep $k = 1, 2$ in Eq. (4) only with

$$I_{kj} = -4eT_c (-1)^k k \sum_v (\Delta/2\omega_v)^{2k} e^{-2k\omega_v/E_{Lj}}. \quad (12)$$

In the limit $L \rightarrow 0$ or $E_{Lj} \rightarrow \infty$, both pseudo-spin bands yield supercurrents of the same magnitude, i.e., $\delta I_k = 0$. Thus, the finite length has to be taken into account in order to obtain a diode effect. In a short junction, with logarithmic accuracy, this yields

$$I_{1j} \approx \frac{\pi^2}{2} eT_c \left(\frac{\Delta}{2\pi T_c} \right)^2 \left(1 - \frac{4}{\pi^2} \frac{2\pi T_c}{E_{Lj}} \ln \frac{E_{Lj}}{2\pi T_c} \right), \quad (13)$$

$$I_{2j} \approx -\frac{\pi^2}{24} eT_c \left(\frac{\Delta}{2\pi T_c} \right)^4. \quad (14)$$

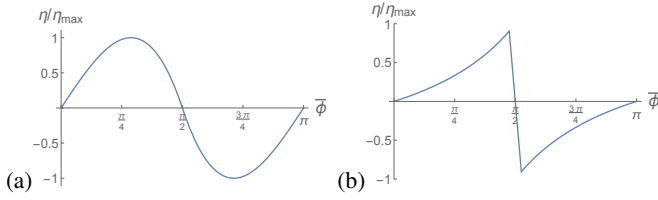


FIG. 2. The diode efficiency at $T = 0$ due to the magnetic field in the junction as a function of the phase shift $\bar{\phi} \propto \bar{h}$ for (a) a short junction and (b) a long junction. In the latter case, the width of the phase interval around $\pi/2$ where η decreases with $\bar{\phi}$ is set by $\delta v/\bar{v}$.

Thus $I_{c2}/I_{c1} \approx -(\Delta/2\pi T_c)^2/12$ and

$$\delta_{12} \approx -\frac{4}{\pi^2} \frac{2\pi T_c}{\bar{E}_L} \ln\left(\frac{\bar{E}_L}{2\pi T_c}\right) \frac{\delta v}{\bar{v}} \frac{\bar{h}}{\bar{E}_L} \ll 1. \quad (15)$$

The diode efficiency η_{short} is then given by Eq. (9).

In a long junction, the contributions from Matsubara frequencies $\omega_{v>0}$ are suppressed when $E_{Lj} \ll T \ll T_c$ and we may approximate $a(\omega_0) \approx -1$. As a consequence, $I_{kj} \propto \exp[-k2\pi T/E_{Lj}]$ and we may keep $k = 1, 2$ in Eq. (4) only with

$$I_{kj} \approx -4eT(-1)^k k e^{-k2\pi T/E_{Lj}}. \quad (16)$$

At small \bar{h} , this yields

$$\delta_{12} \approx \left(\tanh \frac{2\pi T \delta v}{\bar{E}_L \bar{v}} - \tanh \frac{\pi T \delta v}{\bar{E}_L \bar{v}} \right) \frac{2\bar{h}}{\bar{E}_L}. \quad (17)$$

At $\delta v/\bar{v} \ll \bar{E}_L/T$, the result simplifies to $\delta_{12} \approx -2\pi(T\bar{h}/\bar{E}_L^2)\delta v/\bar{v} \ll 1$. The corresponding diode efficiency is exponentially suppressed, $\eta_{\text{long}} \propto \exp[-2\pi T/\bar{E}_L]$.

Though the current-phase relation of a ballistic Josephson junction at $T = 0$ contains many harmonics and displays jumps, analytical results can be obtained both for short and long junctions.

To obtain a diode effect in a short junction, we need to keep both the phase acquired in the junction ($\propto h_j L$) and the leading correction in $\Delta/E_{Lj} \ll 1$. While the main contribution to the Josephson current is carried by Andreev bound states with energy $E_{Aj} = \Delta \cos((\phi + j\phi_j)/2)$, the correction comes from the continuum³⁸, which carries a current in the opposite direction. With logarithmic accuracy, one finds

$$I_j = \frac{e\Delta}{2} \sum_{j=\pm} \sin \frac{\phi + j\phi_j}{2} \text{sign} \left(\cos \frac{\phi + j\phi_j}{2} \right) \times \left[1 - \frac{4}{\pi} \left(\frac{\Delta}{E_{Lj}} \ln \frac{E_{Lj}}{\Delta} \right) \left| \cos \frac{\phi + j\phi_j}{2} \right| \right]. \quad (18)$$

Thus, we find an average critical current $\bar{I}_c = (e\Delta/2)(1 + |\cos \bar{\phi}|)$ and a diode efficiency

$$\eta_{0\text{short}} = \frac{2}{\pi} \left(\frac{\Delta}{\bar{E}_L} \ln \frac{\bar{E}_L}{\Delta} \right) \frac{\delta v}{\bar{v}} \frac{\sin(2\bar{\phi})}{1 + |\cos \bar{\phi}|}. \quad (19)$$

The maximal diode efficiency is $\eta_{0\text{short}}^{\text{max}} = \sqrt{10\sqrt{5} - 22} (2\Delta\delta v/\pi\bar{E}_L\bar{v}) \ln(\bar{E}_L/\Delta)$. The dependence on $\bar{\phi}$ is shown in Fig. 2(a).

In a long Josephson junction, the current-phase relation at $T = 0$ of each pseudo-spin band has a sawtooth shape³⁹. The total current reads

$$I_j = \sum_{j=\pm} eE_{Lj} \left[\frac{\phi + j\phi_j}{2\pi} - \text{Int} \left(\frac{\phi + j\phi_j + \pi \text{sign}(\phi + j\phi_j)}{2\pi} \right) \right]. \quad (20)$$

Defining $x = \bar{\phi}/\pi - \text{Int}(\bar{\phi}/\pi)$, this yields an average critical current

$$\bar{I}_c = e\bar{E}_L \begin{cases} 1-x, & x < \frac{1}{2}(1 - \frac{\delta v}{2\bar{v}}), \\ \frac{1}{2}(1 + \frac{\delta v}{2\bar{v}}), & \frac{1}{2}(1 - \frac{\delta v}{2\bar{v}}) < x < \frac{1}{2}(1 + \frac{\delta v}{2\bar{v}}), \\ x, & \frac{1}{2}(1 + \frac{\delta v}{2\bar{v}}) < x, \end{cases} \quad (21)$$

and a diode efficiency

$$\eta_{0\text{long}} \approx \begin{cases} \frac{\delta v}{2\bar{v}} \frac{x}{1-x}, & x < \frac{1}{2}(1 - \frac{\delta v}{2\bar{v}}), \\ 1-2x, & \frac{1}{2}(1 - \frac{\delta v}{2\bar{v}}) < x < \frac{1}{2}(1 + \frac{\delta v}{2\bar{v}}), \\ -\frac{\delta v}{2\bar{v}} \frac{1-x}{x}, & \frac{1}{2}(1 + \frac{\delta v}{2\bar{v}}) < x. \end{cases} \quad (22)$$

The maximal diode efficiency is $\eta_{0\text{long}}^{\text{max}} = \delta v/(2\bar{v}) \gg \eta_{0\text{short}}^{\text{max}}$. I.e., the diode efficiency is enhanced in a long junction. The dependence on $\bar{\phi}$ is shown in Fig. 2(b).

We finally turn to the effect of the magnetic field in the leads. As shown in Ref. 34, the magnetic field h_j^S yields a diode effect in a topological junction where only one pseudo-spin band is present. It is due to the fact that the magnetic field induces a current in the leads, which are formed of helical edges “proximitized” by a conventional superconductor. Indeed, if superconductivity in the edges were intrinsic, the field would induce a spatially modulated order parameter corresponding to a zero-current state. By contrast, the uniform order parameter imposed by the conventional superconductor covering the edges forces a current along the edges and, thus, across the junction. In the short junction limit, $L \rightarrow 0$, and $h \equiv h_j^S < \Delta$, the current-phase relation of a single pseudo-spin band at $T = 0$ reads^{34,40}

$$I_j(\phi) = \frac{eh}{\pi} + \frac{e\Delta}{2} \sin \frac{\phi}{2} \text{sign} \left(\cos \frac{\phi + j\phi_j}{2} \right), \quad (23)$$

where $\phi_j = 2 \arcsin(h_j^S/\Delta)$. The diode efficiency is given as

$$\eta_{\text{topo}}^S = \frac{4h/\pi\Delta - 1 + \sqrt{1 - h^2/\Delta^2}}{1 + \sqrt{1 - h^2/\Delta^2}}. \quad (24)$$

Its maximum value $\eta_{\text{topo}}^{\text{max}} = 4/\pi^2$ is achieved at $h/\Delta = 4\pi/(\pi^2 + 4)$. In the presence of both pseudo-spin bands, there is a partial cancellation between the bands as the currents they carry in the leads are opposed²⁸. The residual diode efficiency is given as⁴³

$$\eta^S = \begin{cases} \frac{2\delta h}{\pi\Delta} - \frac{\sqrt{1 - h_-^2/\Delta^2} + \sqrt{1 - h_+^2/\Delta^2}}{\sqrt{1 - h_-^2/\Delta^2} + \sqrt{1 - h_+^2/\Delta^2}} & \frac{h_-}{\Delta_-} < \sqrt{1 - \frac{\delta\Delta^2}{4\Delta^2}} \\ \frac{2\delta h}{\pi\Delta} - \frac{\delta\Delta/(2\Delta) + \sqrt{1 - h_-^2/\Delta^2}}{\delta\Delta/(2\Delta) + \sqrt{1 - h_+^2/\Delta^2}} & \sqrt{1 - \frac{\delta\Delta^2}{4\Delta^2}} < \frac{h_-}{\Delta_-} < 1 \end{cases} \quad (25)$$

Using $h_+/\Delta_+ = h_-/\Delta_- \equiv h/\Delta$, we find a maximal diode efficiency $\eta_{\max}^S = (2/\pi)\sqrt{1 - \delta\Delta^2/(4\bar{\Delta}^2)}$ at $h/\Delta = \sqrt{1 - \delta\Delta^2/(4\bar{\Delta}^2)}$.

A finite length of the junction or finite temperature both suppress the diode efficiency as can be checked numerically using Eq. (3).

In all of the above results, the limiting factor for the diode efficiency is the Fermi velocity asymmetry. Using typical parameters for InSb⁴⁵ ($E_{so} \sim 5\text{meV}$, $\bar{\mu} \sim m\omega_0^2/2 \sim 20\text{meV}$), we estimate $\delta v/\bar{v}$ due to the finite width of the nanowire of the order of 10^{-2} far from avoided crossings. By tuning the chemical potential, much larger asymmetries should be achievable. When the asymmetry is induced by a magnetic field, values of $\delta v/\bar{v}$ of the order of 10^{-1} should be reached at fields $B_\perp \sim 1\text{T}$ taking $g \sim 40$.

In conclusion, we presented a simple model for a Josephson diode effect in a single-channel ballistic nanowire with Rashba spin-orbit coupling and subject to a Zeeman field. The diode effect arises due to the interplay between the Andreev bound states forming within the two pseudo-spin bands. We derived microscopically the current-phase relation that was used phenomenologically in previous works. We showed that the diode effect induced by the magnetic field has two different contributions. One contribution is due to the field in the junction; it increases with the length of the junction. Another contribution is due to the field in the leads; it is maximal in a short junction when only one pseudo-spin band is present. In general, both contributions may be present. While their relative strength will depend on the details of magnetic screening, the length of the junction is crucial in determining which one is dominant based on the discussion above. The general result, Eq. (3), allows on to compute the current-phase relation including both effects. The same physical ingredients also yield an anomalous Josephson current^{16,17,19–21,46}. We discuss connections and differences between the two effects in the Supplementary Material. The experimental challenge is to separate the diode effect due to the interplay between spin-orbit coupling and a Zeeman field from other origins. The predictions given in this work can serve as a guide for assessing the microscopic origin of the diode effect in a concrete setup.

ACKNOWLEDGMENTS

We thank Liang Fu and Jean-Damien Pillet for interesting exchanges. Furthermore, we thank Alessandro De Martino for pointing out an error in the estimation of the velocity mismatch. We wish to acknowledge funding from the French Agence Nationale de la Recherche through Grants No. ANR-17-PIRE-0001 (HYBRID) and ANR-21-CE30-

0035 (TRIPRES).

Appendix A: 2D harmonic nanowire with Rashba spin-orbit coupling

Here we provide a simple twodimensional model of a nanowire with Rashba spin-orbit coupling^{24,25}. The confining potential along the y -direction is considered harmonic with frequency ω_0 , $V(y) = m\omega_0^2 y^2/2$, where m is the effective electron mass. Furthermore, we include an in-plane magnetic field $\vec{h} = h_x\vec{u}_x + h_y\vec{u}_y$. The Hamiltonian takes the form

$$H = \frac{\vec{p}^2}{2m} + \frac{1}{2}m\omega_0^2 y^2 - \alpha(\vec{p} \times \vec{\sigma}) \cdot \vec{u}_z + \vec{h} \cdot \vec{\sigma}, \quad (\text{S1})$$

where $\vec{p} = (p_x, p_y)$ is the in-plane momentum, α is the strength of the Rashba spin-orbit coupling, σ_i ($i = x, y, z$) are Pauli matrices in spin space, and \vec{u}_z is a unit vector perpendicular to the plane.

We will consider the transverse spin-orbit coupling ($\sim \alpha p_y$) as well as the field along the wire (h_x) as perturbations, namely we will assume $\alpha p_y, h_x \ll \omega_0$. The Hamiltonian

$$H_0 = \frac{\vec{p}^2}{2m} + \frac{1}{2}m\omega_0^2 y^2 - \alpha p_x \sigma_y + h_y \sigma_y \quad (\text{S2})$$

can be easily diagonalized. The eigenfunctions take the form

$$\Psi_{k_x, n, \pm}(x, y) = e^{ik_x x} \chi_n(y) \frac{1}{\sqrt{2}} \begin{pmatrix} 1 \\ \pm i \end{pmatrix}, \quad (\text{S3})$$

where $\chi_n(y)$ are the harmonic oscillator eigenfunctions, with eigenenergies

$$E_{n\pm}(k_x) = \frac{k_x^2}{2m} + \omega_0(n + \frac{1}{2}) - \mu \mp (\alpha k_x - h_y). \quad (\text{S4})$$

Note that the spin states within a subband have the same velocity at a given energy. Band crossings between the two spin states in the first subband take place at $k_x = h_y/\alpha$. Band crossings between opposite spin states in the first and second subband take place at $k_x = \mp \omega_0/(2\alpha) + h_y/\alpha$. The transverse spin-orbit coupling and the longitudinal magnetic field open gaps at these crossings and thus modify the velocities of the different bands and change the spin-projection of the eigenstates. For sufficiently low chemical potential, we may write an effective Hamiltonian in the space spanned by $\Psi_{k_x, 0, +}$, $\Psi_{k_x, 0, -}$, $\Psi_{k_x, 1, +}$, $\Psi_{k_x, 1, -}$, namely

$$\tilde{H} = \frac{k_x^2}{2m} - (\alpha k_x - h_y)\sigma_z - \omega_0(1 - \frac{1}{2}\eta_z) + \eta\sigma_y\eta_y + h_x\sigma_y - \mu \quad (\text{S5})$$

with $\eta = \alpha\sqrt{m\omega_0/2} \equiv \sqrt{E_{so}\omega_0}$. The spectrum is given as

$$E_{s_1 s_2} = \frac{k_x^2}{2m} + \omega_0 - \mu + s_1 \sqrt{(\alpha k_x - h_y)^2 + h_x^2 + \frac{\omega_0^2}{4} + \eta^2} + s_2 \sqrt{(\alpha k_x - h_y)^2 \omega_0^2 + 4h_x^2 \left(\frac{\omega_0^2}{4} + \eta^2\right)}. \quad (S6)$$

Unless the chemical potential is close to an avoided crossing, we may approximate the two lowest bands as

$$E_{\pm} \approx \frac{(k_x \mp m\alpha)^2}{2m} + \frac{\omega_0}{2} - \mu - \frac{m\alpha^2}{2} \mp \left(\frac{h_x^2}{2\alpha k_x} + \frac{\eta^2}{2\alpha k_x \pm \omega_0} \right) \mp h_y \left(1 - \frac{h_x^2}{2\alpha^2 k_x^2} - \frac{\eta^2}{(2\alpha k_x \pm \omega_0)^2} \right). \quad (S7)$$

The Fermi momenta are obtained by setting $E_{\pm}(k_F^{\pm}, h_y = 0) = 0$ whereas the Fermi velocities are obtained as

$$v_{\pm} = \frac{\partial E_{\pm}(k_x, h_y = 0)}{\partial k_x} \Big|_{k_x = k_F^{\pm}} = \frac{k_F^{\pm}}{m} \mp \alpha \pm \left(\frac{h_x^2}{2\alpha(k_F^{\pm})^2} + \frac{2\alpha\eta^2}{(2\alpha k_F^{\pm} \pm \omega_0)^2} \right).$$

Let us consider the effect of η first. At weak spin-orbit coupling, we may develop

$$E_{\pm}(k_x, h_x = h_y = 0) \approx \frac{(k_x \mp m\alpha)^2}{2m} + \frac{\omega_0}{2} - \mu - \frac{m\alpha^2}{2} - \frac{\eta^2}{\omega_0} \left(1 \mp \frac{2\alpha k_x}{\omega_0} + \left(\frac{2\alpha k_x}{\omega_0} \right)^2 \mp \left(\frac{2\alpha k_x}{\omega_0} \right)^3 \right). \quad (S8)$$

Only the last term contributes to an asymmetry in the velocities. Namely

$$v_{\pm} = \bar{v} \pm \frac{8\eta^2 \alpha^3 \bar{k}_F^2}{\omega_0^4}. \quad (S9)$$

Here $\bar{v} = \bar{k}_F/m$ and $\bar{k}_F \approx \sqrt{2m(\mu - \frac{\omega_0}{2})}$. The effective fields are given as

$$h_{\pm} \approx h_y \left(1 \pm \frac{2\eta^2 \alpha \bar{k}_F}{\omega_0^3} \right), \quad (S10)$$

where we neglected the suppression of \bar{h} . Taking it into account, one recovers $h_{\pm} \leq h_y$. Note that $\delta v/\bar{v} \ll \delta h/\bar{h}$.

We now turn to the effect of h_x . With $k_F^{\pm} \approx \bar{k}_F \pm m\alpha$, we find

$$v_{\pm} \approx \bar{v} \pm \frac{h_x^2}{2\alpha \bar{k}_F^2} \quad (S11)$$

and

$$h_{\pm} \approx h_y \left(1 \pm \frac{mh_x^2}{\alpha \bar{k}_F^3} \right). \quad (S12)$$

Here both $\delta v/\bar{v}, \delta h/\bar{h} \sim h_x^2 m/(\alpha \bar{k}_F^3)$.

Appendix B: Anomalous Josephson effect

The so-called anomalous Josephson effect, i.e., the presence of Josephson current in the absence of an applied phase difference ($\phi = 0$), arises from the same interplay between spin-orbit coupling and an external magnetic field. In contrast to the diode effect, a current-phase relation with a single harmonic is sufficient to obtain an anomalous Josephson current. The anomalous Josephson effect due to the magnetic field in

the leads has been studied in detail in Refs. 28 and 34. Here we provide results for the anomalous Josephson current due to the field within the junction. For a current-phase relation dominated by the first harmonic, it is given as $I_{an} \approx -I_{c1} \sin(\phi_{01})$, except for phases $\phi_{01} \approx n\pi$, where the higher harmonics come into play. At small fields, the anomalous current is linear in \bar{h} and given as

$$I_{an} \approx \bar{I}_1 \delta\phi + \delta I_1 \bar{\phi}. \quad (S13)$$

With this, we can compute the anomalous current for a short junction close to T_c . It is dominated by the first term in Eq. (S13) yielding

$$I_{an}^{\text{short}} \approx \frac{e\Delta^2}{8T_c} \frac{\bar{h}}{\bar{E}_L} \left(\frac{\delta h}{\bar{h}} - \frac{\delta v}{\bar{v}} \right). \quad (S14)$$

Eq. (S13) also gives the anomalous Josephson current in a long junction at $T \gg \bar{E}_L$, namely

$$I_{an}^{\text{long}} \approx 4eT e^{-2\pi T/\bar{E}_L} \left(\delta\phi \cosh \frac{\pi T \delta v}{\bar{E}_L \bar{v}} + \bar{\phi} \sinh \frac{\pi T \delta v}{\bar{E}_L \bar{v}} \right). \quad (S15)$$

We note that in both cases $|I_{an}| \gg |I_c^> - I_c^<| \propto \bar{I}_2$.

At $T = 0$, the situation is a little more subtle. The anomalous current of a short junction is given as

$$I_{an}^{0\text{short}} \approx -\frac{e\Delta}{2} \sum_{j=\pm} j \sin \frac{\phi_j}{2} \text{sign} \left[\cos \frac{\phi_j}{2} \right]. \quad (S16)$$

To lowest order in field, one obtains $I_{an} \approx -e\Delta \delta\phi/4$. In the narrow interval $\bar{\phi} - \delta\phi/2 < (2n+1)\pi < \bar{\phi} + \delta\phi/2$, the anomalous current is strongly enhanced reaching values comparable to the critical current, $I_{an} \sim e\Delta$. In a long junction, the anomalous current to lowest order in the field is given as

$$I_{an}^{0\text{long}} = -e\bar{E}_L \left(\frac{\delta\phi}{2\pi} + \frac{\delta v}{\bar{v}} \frac{\bar{\phi}}{2\pi} \right). \quad (S17)$$

As in the short junction case, in the narrow interval $\bar{\phi} - \delta\phi/2 < (2n+1)\pi < \bar{\phi} + \delta\phi/2$, the anomalous current is strongly enhanced reaching values comparable to the critical current, $I_{an} \sim e\bar{E}_L$.

- ¹M. Nadeem, M.S. Fuhrer, and X. Wang, *Nature Reviews Physics* **5**, 558 (2023).
- ²N. Nagaosa, and Y. Yanase, *Annual Review of Condensed Matter Physics* **15**, 63 (2024).
- ³F. Ando, Y. Miyasaka, T. Li *et al.*, *Nature* **584**, 373 (2020).
- ⁴L. Bauriedl, C. Bäuml, L. Fuchs *et al.*, *Nat Commun* **13**, 4266 (2022).
- ⁵J.X. Lin, P. Siriviboon, H.D. Scammell *et al.*, *Nat. Phys.* **18**, 1221 (2022).
- ⁶N. Satchell, P.M. Shepley, M.C. Rosamond, and G. Burnell, *Journal of Applied Physics* **133**, 203901 (2023).
- ⁷Y. Hou, F. Nichele, H. Chi *et al.*, *Phys. Rev. Lett.* **131**, 027001 (2023).
- ⁸C. Baumgartner, L. Fuchs, A. Costa *et al.*, *Nat. Nanotechnol.* **17**, 39 (2022).
- ⁹B. Pal, A. Chakraborty, P.K. Sivakumar *et al.*, *Nat. Phys.* **18**, 1228 (2022).
- ¹⁰T.A. Fulton, L. N. Dunkleberger, and R.C. Dynes, *Phys. Rev. B* **6**, 855 (1972).
- ¹¹H. Wu, Y. Wang, Y. Xu *et al.*, *Nature* **604**, 653 (2022).
- ¹²J. Díez-Mérida, A. Díez-Carlón, S.Y. Yang *et al.*, *Nat Commun* **14**, 2396 (2023).
- ¹³M. Trahms, L. Melischek, J.F. Steiner *et al.*, *Nature* **615**, 628 (2023).
- ¹⁴J. Chiles, E.G. Arnault, C.-C. Chen *et al.*, *Nano Lett.* **23**, 5257 (2023).
- ¹⁵B. Zhang, Z. Li, V. Aguilar *et al.*, preprint arXiv:2212.00199.
- ¹⁶A.A. Reynoso, G. Usaj, C.A. Balseiro, D. Feinberg, and M. Avignon, *Phys. Rev. Lett.* **101**, 107001 (2008).
- ¹⁷A.A. Reynoso, G. Usaj, C.A. Balseiro, D. Feinberg, and M. Avignon, *Phys. Rev. B* **86**, 214519 (2012).
- ¹⁸T. Yokoyama, M. Eto, and Y.V. Nazarov, *Phys. Rev. B* **89**, 195407 (2014).
- ¹⁹V.B. Geshkenbein and A.I. Larkin, *Pis'ma Zh. Eksp. Teor. Fiz.* **43**, 306 (1986) [*JETP Lett.* **43**, 395 (1986)].
- ²⁰I.V. Krive, L.Y. Gorelik, R.I. Shekhter, and M. Jonson, *Fiz. Nizk. Temp.* **30**, 535 (2004) [*Low Temp. Phys.* **30**, 398 (2004)].
- ²¹A.I. Buzdin, *Phys. Rev. Lett.* **101**, 107005 (2008).
- ²²J.-X. Hu, Z.-T. Sun, Y.-M. Xie, and K. T. Law, *Phys. Rev. Lett.* **130**, 266003 (2023).
- ²³P.A. Volkov, E. Lantagne-Hurtubise, T. Tummuru, S. Plugge, J.H. Pixley, and M. Franz, *Phys. Rev. B* **109**, 094518 (2024)..
- ²⁴M. Governale and U. Zülicke, *Phys. Rev. B* **66**, 073311 (2002).
- ²⁵S. Park and A. L. Yeyati, *Phys. Rev. B* **96**, 125416 (2017).
- ²⁶R.M. Lutchyn, J.D. Sau, and S. Das Sarma, *Phys. Rev. Lett.* **105**, 077001 (2010).
- ²⁷Y. Oreg, G. Refael, and F. von Oppen, *Phys. Rev. Lett.* **105**, 177002 (2010).
- ²⁸K.N. Nesterov, M. Houzet, and J.S. Meyer, *Phys. Rev. B* **93**, 174502 (2016).
- ²⁹In a 3D nanowire, typically $a \sim \lambda_F$: in that case, the orbital effect needs to be taken into account for a quantitative prediction of the diode effect at the optimal field.
- ³⁰The magnetic field in the leads may also affect the induced superconductivity, leading to different gaps Δ_{\pm} in the two pseudo-spin bands. Here we neglect this effect.
- ³¹T. de Picoli, Z. Blood, Y. Lyanda-Geller, and J.I. Väyrynen *Phys. Rev. B* **107**, 224518 (2023).
- ³²S.J. De, U. Khanna, S. Rao, and S. Das, *Phys. Rev. B* **108**, L161403 (2023).
- ³³J. Cayao, N. Nagaosa, and Y. Tanaka *Phys. Rev. B* **109**, L081405 (2024).
- ³⁴F. Dolcini, M. Houzet, and J.S. Meyer, *Phys. Rev. B* **92**, 035428 (2015).
- ³⁵Note that the same equations may also be used to describe an asymmetric SQUID^{36,37}, where the subscript j labels the two Josephson junctions in the SQUID loop and $\phi_j = j\Phi/(2\Phi_0)$ with Φ the flux through the loop.
- ³⁶Ya.V. Fominov and D.S. Mikhailov, *Phys. Rev. B* **106**, 134514 (2022).
- ³⁷R.S. Souto, M. Leijnse, and C. Schrade, *Phys. Rev. Lett.* **129**, 267702 (2022).
- ³⁸A. Levchenko, A. Kamenev, and L.I. Glazman, *Phys. Rev. B* **74**, 212509 (2006).
- ³⁹C. Ishii, *Prog. Theor. Physics* **44**, 1525 (1970).
- ⁴⁰One obtains the same current-phase relation when finite-momentum pairing is realized in the conventional superconducting leads^{41,42}.
- ⁴¹A. Zazunov, J. Rech, T. Jonckheere, B. Grémaud, T. Martin, and R. Egger, *Phys. Rev. B* **109**, 024504 (2024).
- ⁴²M. Davydova, S. Prembabu, and L. Fu, *Science Advances* **8**, eabo0309 (2022).
- ⁴³Similar results for the case $\Delta_+ = \Delta_-$ were obtained in Ref. 44.
- ⁴⁴P.-H. Fu, Y. Xu, S.A. Yang, C.H. Lee, Y.S. Ang, and J.-F. Liu, *Phys. Rev. Applied* **321**, 054057 (2024).
- ⁴⁵J. Kammhuber, M.C. Cassidy, F. Pei *et al.*, *Nature Communications* **8**, 478 (2017).
- ⁴⁶R.D. Monaghan and G.C. Tettamanzi, preprint arXiv:2403.05052.